

Cite this: *Chem. Sci.*, 2017, **8**, 2914

Mechanistic insights on the Pd-catalyzed addition of C–X bonds across alkynes – a combined experimental and computational study†

Theresa Sperger,^a Christine M. Le,^b Mark Lautens^{*b} and Franziska Schoenebeck^{*a}

The Pd-catalyzed intramolecular addition of carbamoyl chlorides and aryl halides across alkynes is investigated by means of DFT calculations and mechanistic test experiments. The data suggest a mechanistic pathway that involves oxidative addition, alkyne insertion, *cis* → *trans* isomerization and reductive elimination. Our data indicate that oxidative addition is the reactivity limiting step in the addition of aryl chlorides and bromides across alkynes. However, for the corresponding addition of carbamoyl chlorides, alkyne insertion is found to be limiting. Full energetic reaction pathways for the intramolecular additions across alkynes are presented herein and the role of ligands, alkyne substituents and tether moieties are discussed. Notably, the calculations could rationalize a pronounced effect of the alkyne substituent, which accounts for the exceptional reactivity of TIPS-substituted alkynes. In particular, the bulky silyl moiety is shown to significantly destabilize the formed Pd(II)-intermediates, thus facilitating both *cis* → *trans* isomerization and reductive elimination, which overall results in a flatter energetic landscape and a therefore increased catalytic efficiency.

Received 12th November 2016
Accepted 26th January 2017

DOI: 10.1039/c6sc05001h
rsc.li/chemical-science

Introduction

Methylene oxindoles are a highly relevant motif in many biologically active molecules and natural products.^{1–8} Despite their use in medicinal chemistry and natural product synthesis, methods to access methylene oxindoles in a highly stereoselective manner are limited.^{9–15} In this context, Lautens and co-workers have developed the synthesis of methylene oxindoles *via* Pd(0)-catalyzed carbohalogenation of alkynes, which involves an unusual and remarkable reductive elimination of C(sp²)-X (X = I, Br, Cl) from Pd(II) as key step.¹⁶

While oxidative additions of aryl and vinyl halides to Pd(0) are widely studied and a relatively well understood step in Pd-catalysis, the corresponding back reaction, *i.e.* the reductive elimination of C–X bonds from Pd(II) has had significantly less precedence.¹⁷ A reason for this is that reductive elimination from Pd(II) is generally slow and disfavored. Therefore, chemists have turned to alternative protocols, *e.g.* oxidatively accessing the reductive elimination from higher oxidation state Pd intermediates, such as Pd(III) and Pd(IV).^{18–27} However, C–X bond

formation *via* reductive elimination from Pd(II) may become feasible under sterically demanding conditions (bulky ligands and substituents) and if potential side-reactions are suppressed (substrate control, *e.g.* avoiding the β -H elimination).^{28–32} Advances in substrate design as well as catalyst development by the Lautens group recently allowed for the reductive elimination of C(sp²)-X (X = I, Br, Cl) from Pd(II) in the carbohalogenation of alkynes (Scheme 1).¹⁶ Interestingly, the synthetic protocol was compatible with ether, alkyl and amine tethers (Scheme 1, 1), but the use of an amide tether (4) required an alternative synthetic route *via* the chlorocarbamoylation of alkynes.¹⁵ This complementary synthesis utilizes the reactivity of carbamoyl chlorides, a relatively underexplored class of substrates. In contrast to the original synthetic method which employs aryl halides (1) in combination with bulky phosphines, such as Q-Phos and PtBu₃, the use of carbamoyl chlorides (3) required a less bulky aryl phosphadamatane ligand (PA-Ph = 1,3,5,7-tetramethyl-2,4,8-trioxa-6-phenyl-6-phosphadamatane) in order to reach good conversions. Furthermore, the chlorocarbamoylation reaction (Scheme 1b) exclusively allows for a bulky tri-iso-propylsilyl (TIPS) alkyne substituent, but is not effective using less bulky silyls or bulky aryl moieties (such as Mes = mesityl). This is in contrast to the carbohalogenation reaction (Scheme 1a) that displays good yields for a number of aryl halides with either bulky silyl or aryl alkyne substituents (*e.g.* TIPS, TBS = *tert*-butyldimethylsilyl, Mes, 1-naphthyl, 9-anthracenyl).

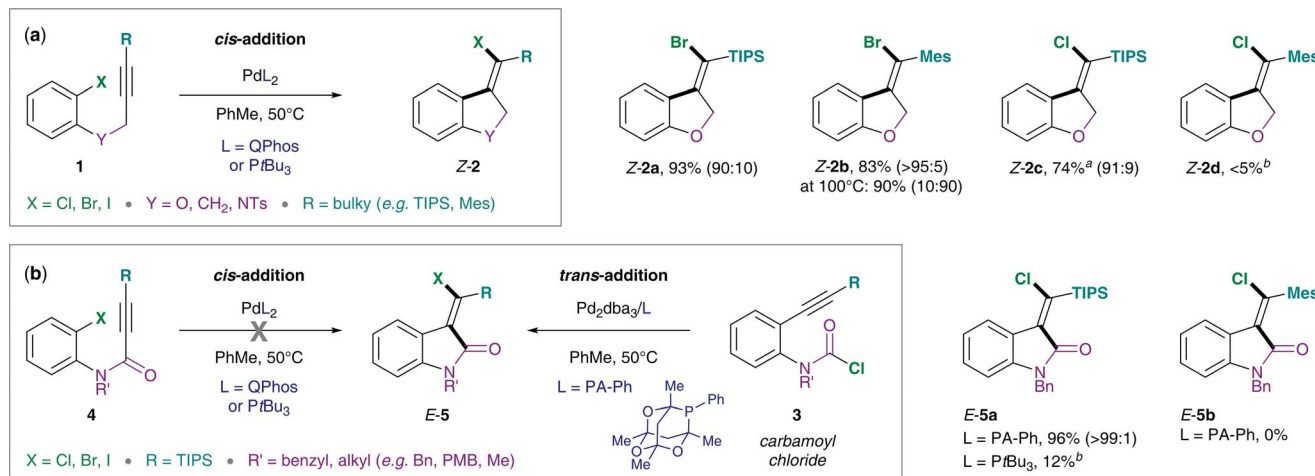
Herein we present a combined computational and experimental study in an effort to understand the underlying

^aRWTH Aachen University, Institute of Organic Chemistry, Landoltweg 1, 52074 Aachen, Germany. E-mail: franziska.schoenebeck@rwth-aachen.de

^bUniversity of Toronto, Davenport Laboratories, Department of Chemistry, 80 St. George Street, Toronto, Ontario M5S 3H6, Canada. E-mail: mlautens@chem.utoronto.ca

† Electronic supplementary information (ESI) available: Computational details, cartesian coordinates of calculated species, experimental procedures, and spectroscopic data are given. See DOI: [10.1039/c6sc05001h](https://doi.org/10.1039/c6sc05001h)





Scheme 1 Experimental data by Lautens and co-workers: (a) intramolecular addition of aryl halides (1) across alkynes,¹⁶ (b) intramolecular addition of carbamoyl chlorides (3) across alkynes.¹⁵ ^aReaction was performed at 110 °C using 1,2,2,6,6-pentamethylpiperidine (PMP, 0.25 equiv.) as an additive.^{16,33} ^bYield was determined by ¹H NMR analysis of the crude reaction mixture using 1,3,5-trimethoxybenzene as an internal standard.

mechanism of these transformations and its implication on reactivity. More specifically, we aim to shed light on selectivity- and reactivity-controlling factors of ligand and substrate and the implicit requirements on alkyne substituent as well phosphine ligand. We hope these results will aid future substrate and catalyst design to further expand the scope of these atom-economic and synthetically relevant Pd-catalyzed intramolecular transformations.

Computational methods

DFT calculations were performed using Gaussian 09, Revision D.01.³⁴ Geometry optimizations and frequency calculations were conducted in the gas-phase at the B3LYP/6-31G(d) level of theory, employing LANL2DZ as an ECP for Pd. All stationary points were verified as either minima or transition states. Additionally, transition states (TSs) were confirmed by following the intrinsic reaction coordinate (IRC) to the corresponding intermediates. Energies were calculated at the M06L/def2-TZVP level of theory, employing the CPCM solvation model to account for toluene as the solvent.³⁵ All energies were converted to 1 M standard state.

Results and discussion

General mechanism

The proposed mechanism of the intramolecular addition of aryl halides and carbamoyl chlorides is shown in Scheme 2. On the basis of our calculations, we propose that initial oxidative addition of either aryl halide 1 or carbamoyl chloride 3 to monophosphine Pd(0) is followed by insertion of the alkyne, *i.e.* *cis*-carbopalladation. Direct reductive elimination (for aryl halide substrates 1) or rapid *cis* → *trans* isomerization and successive reductive elimination (in the case of carbamoyl chloride substrates 3) then yields the observed methylene oxindole products *Z*-2 and *E*-5, respectively.

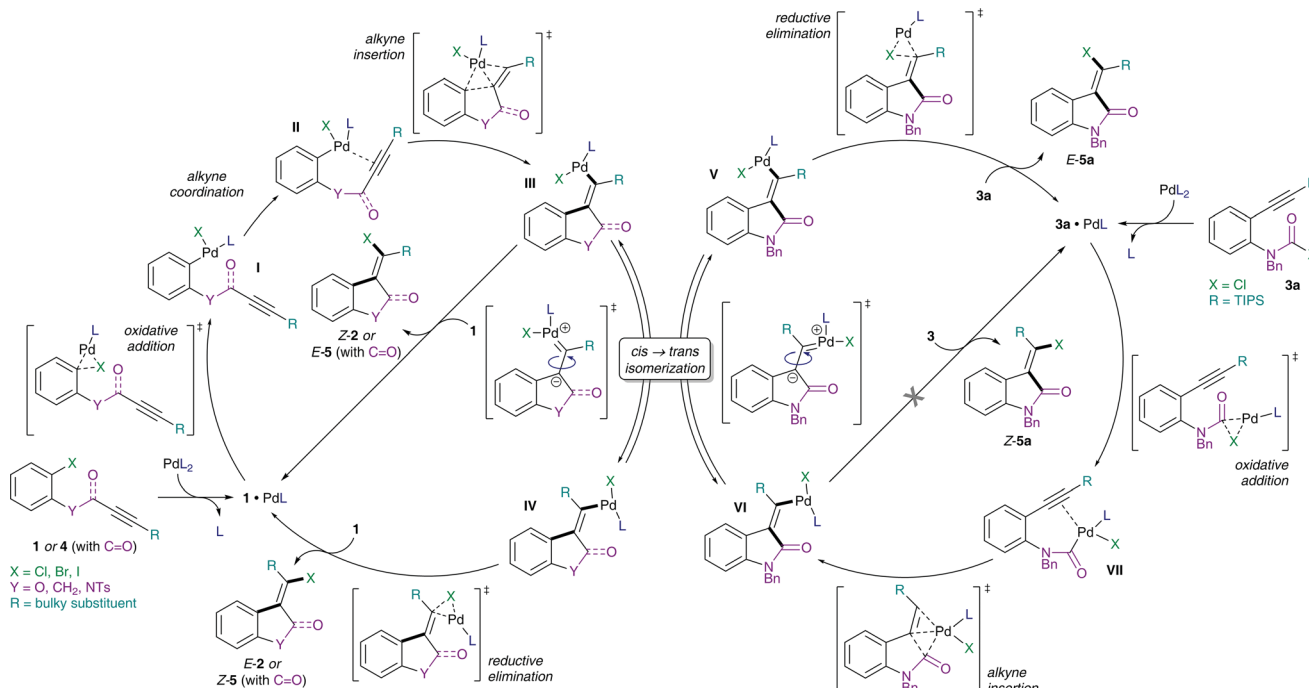
Origin of the superior reactivity of carbamoyl chlorides over aryl chlorides. Our calculations on the intramolecular addition of $\text{C}(\text{sp}^2)\text{-X}$ ($\text{X} = \text{Br}, \text{Cl}$) across alkynes indicate that oxidative addition of aryl halide 1 or 4 is the elementary step with the highest activation barrier (Schemes 2 and 4, left). By contrast, the corresponding intramolecular addition of aryl halides across alkenes proceeds with reductive elimination of the $\text{C}(\text{sp}^3)\text{-X}$ bond ($\text{X} = \text{I}, \text{Br}, \text{Cl}$) as the rate-determining step.^{36,37} In the case of the addition of carbamoyl chlorides across alkynes (see Schemes 2 and 4, right), oxidative addition was found to be the TS with the highest activation barrier when a concerted 3-membered TS geometry was considered.

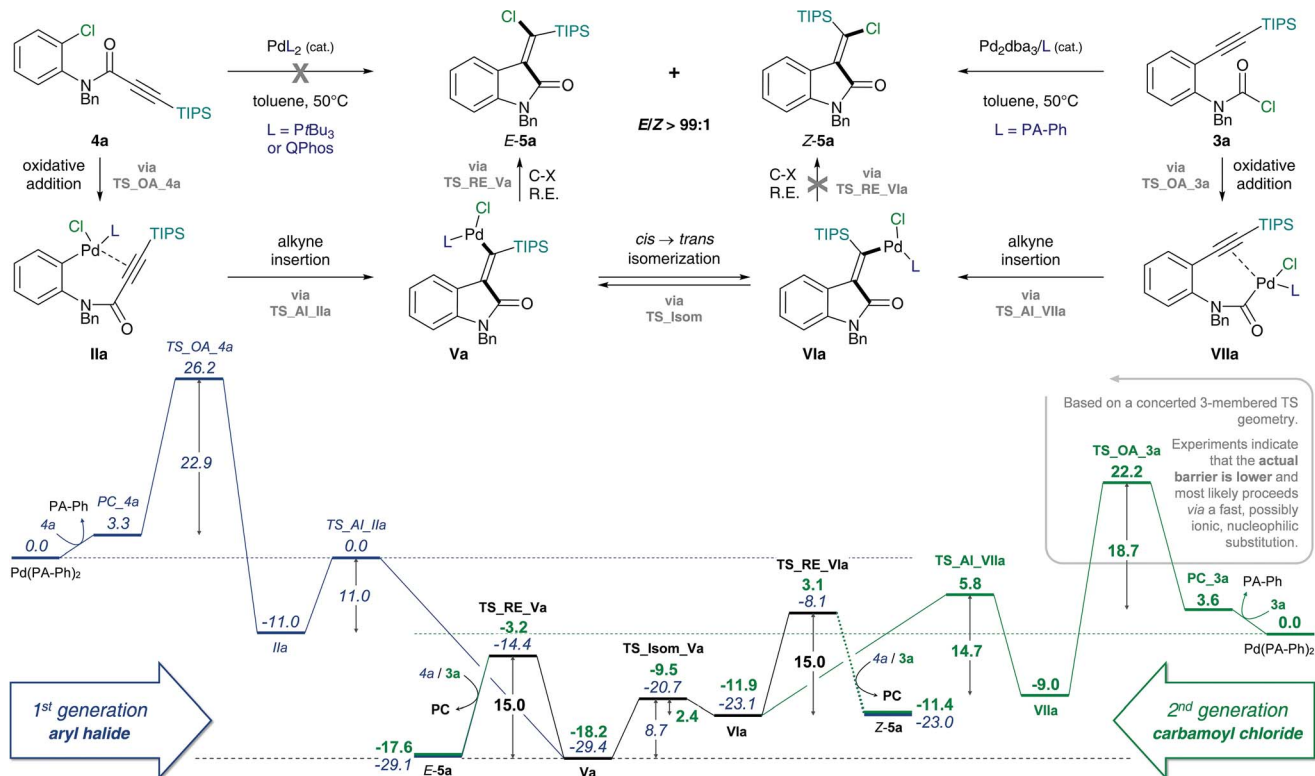
However, while oxidative additions to aryl halides have been subject to extensive computational and mechanistic studies,^{38–45} little is known on the nature of the transition state for reactions with carbamoyl chlorides. The high electrophilicity of these species may imply an ionic/electron transfer or formal nucleophilic substitution reaction. By means of computations it is challenging to unambiguously distinguish between these charged and neutral pathways due to the applied computational approximations.^{46,47}

We therefore designed a test experiment and performed a competitive Suzuki cross-coupling using substrate 6, possessing both aryl chloride and carbamoyl chloride moieties (Scheme 3).⁴⁸ An exclusive activation of carbamoyl chloride over aryl chloride was observed experimentally.⁴⁹

However, despite the clear preference for oxidative addition of carbamoyl chloride over aryl chloride, the arguably fast oxidative addition step (*i.e.* fast compared to oxidative addition to aryl chloride) may still be the rate-determining TS of the reaction. Therefore, a resting state analysis of the reaction of 3a and 4a with catalytic Pd/PA-Ph was performed.⁴⁸ Almost instantaneous conversion of carbamoyl chloride 3a with concomitant formation of new phosphine-containing species and free ligand was observed by ³¹P NMR. In contrast, aryl chloride 4a only yielded traces of product under the same







Scheme 4 Calculated Gibbs free energy pathways of first and second generation substrates **3a** and **4a** possessing an amide tether. Energies (in kcal mol^{-1}) were calculated at the CPCM (toluene) M06L/def2-TZVP//B3LYP/6-31G(d)(LANL2DZ) level of theory. Abbreviations: oxidative addition (OA), alkyne insertion (Al), *cis* \rightarrow *trans* isomerization (Isom) and reductive elimination (RE).

transition states for the oxidative insertion of $\text{Pd}(\text{PA-Ph})$ to potentially activated bonds of substrates **3a** and **4a** were calculated and the corresponding activation barriers compared. In the case of the second generation carbamoyl chloride substrate **3a**, all bond activations are of higher barrier than oxidative addition *via* a concerted, 3-membered TS. Notably, this is despite the fact that experiments indicate an even lower barrier for oxidative addition to the carbamoyl chloride *via* a rapid, possibly ionic, nucleophilic substitution (*vide supra*). In

Table 1 Energetic spans^a and experimental yields of alkyne carbocation and carbamoylation of substrates **3** and **4** bearing an amide tether moiety

Entry	Ligand	Substrate	X	R	$\Delta_r G$	δE	Yield of 5 (ref. 15)
1	PtBu_3	4a	Cl	TIPS	-21.9	28.9	0% (16%) ^b
2	PtBu_3	4b	Cl	Mes	-15.5	45.0	—
3	PA-Ph	4a	Cl	TIPS	-25.8	29.8	—
4	PA-Ph	3a	Cl	TIPS	-14.0	10.0	99%
5	PtBu_3	3a	Cl	TIPS	-10.8	16.4	12%
6	PtBu_3	3b	Cl	Mes	-2.9	38.9	0%

^a Energetic spans (in kcal mol^{-1}) were calculated according to $\delta E = G(\text{TDTS}) - G(\text{TDI}) + \Delta_r G$ (with $G(\text{TDTS})$ = Gibbs free energy of turnover-determining TS, $G(\text{TDI})$ = Gibbs free energy of turnover-determining intermediate, $\Delta_r G$ = Gibbs free energy of reaction), at the CPCM (toluene) M06L/def2-TZVP//B3LYP/6-31G(d)(LANL2DZ) level of theory. ^b Reaction was conducted using stoichiometric amounts of Pd and was heated at 100 °C for 24 h.

contrast, for the first generation aryl chloride substrate **4a**, which did not react under analogous reaction conditions, calculations suggest that an activation of the C-Si bond of the alkyne is competing with oxidative addition to the C-Cl bond. This observation is most likely due to an increase in reactivity of the C-Si bond as a result of the conjugation of the alkyne with the amide.

This activation of the alkyne substituent is not present for all other tether moieties (amine, ether, alkyl), therefore providing a potential explanation for the observed difference in reactivity.

Effect of phosphine ligand. While bulky, electron-rich phosphine ligands such as PtBu_3 and QPhos were well-suited

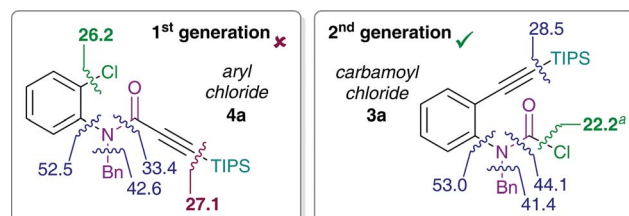


Fig. 1 Activation free energies for insertion of $\text{Pd}(\text{PA-Ph})$ to potentially activated bonds of substrates **4a** (left) and **3a** (right). Values (in kcal mol^{-1}) refer to Gibbs free energies calculated at the CPCM (toluene) M06L/def2-TZVP//B3LYP/6-31G(d)(LANL2DZ) level of theory. ^aCalculated barrier for oxidative addition of carbamoyl chloride *via* a concerted 3-membered TS. Experiments however indicate that the actual barrier is lower and most likely proceeds *via* a fast, possibly ionic, nucleophilic substitution.

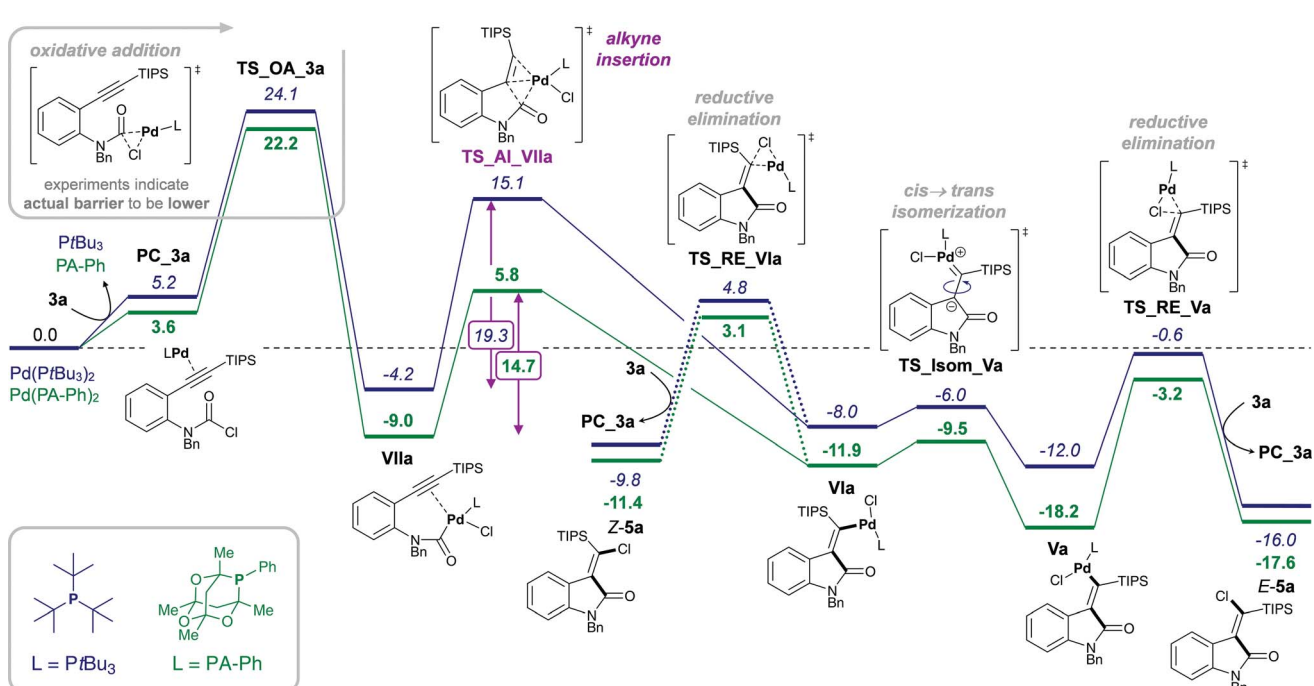
for the addition of aryl halides across alkenes^{36,37} and alkynes¹⁶ (*vide infra*), their use in the addition of carbamoyl chlorides across alkynes only led to small amounts of product being formed. This might be due to the change in TDTS. While oxidative addition is the rate-determining TS for the first generation aryl halide substrate **4**, alkyne insertion was considered to be the TDTS for the second generation carbamoyl chloride substrate **3**. In the case of aryl halide substrate **4**, the bulky PtBu_3 ligand facilitates the reductive elimination of product (Scheme 5), thereby reducing the Gibbs free energy of the reaction ($\Delta_r G$) compared to the corresponding reaction of **4** with the less bulky PA-Ph ligand (Table 1, entries 1 and 3). In contrast, in the case of carbamoyl chloride **3**, the less bulky PA-Ph facilitates the presumed rate-determining alkyne insertion and lowers its activation by approximately 5 kcal mol⁻¹ compared to the corresponding process employing the bulkier PtBu_3 ligand (Scheme 5). This directly causes a significant decrease in energetic span (Table 1, entry 4), thus explaining the superior reactivity observed for PA-Ph in comparison to the bulkier PtBu_3 ligand (entry 5).

Silyl effect

Experimentally, only substrates bearing a silyl-substituent on the alkyne were reactive in the chlorocarbamoylation reaction, whereas substrates with a mesityl-substituted alkyne did not cyclize under analogous reaction conditions. Next, we investigated the role of the alkyne substituent computationally. A significant increase in energetic span for mesityl-substituted substrates **4b** and **3b** (Table 1, entries 2

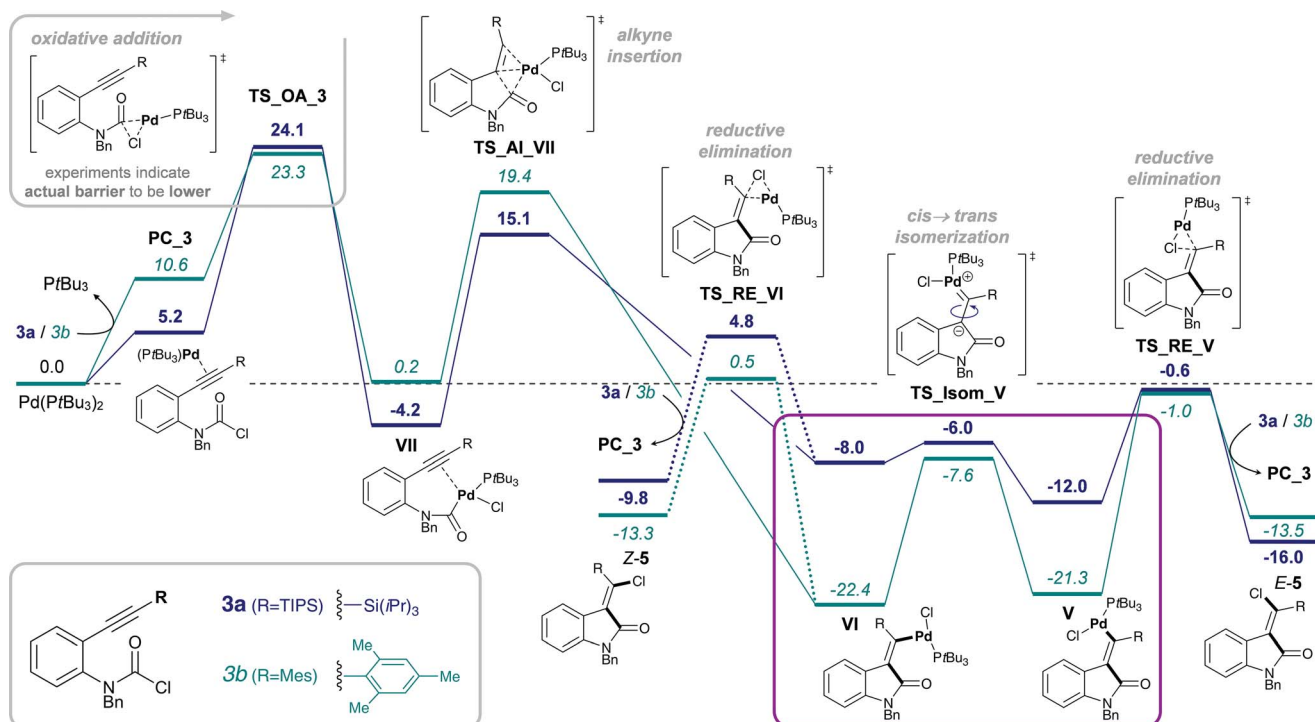
and 6, respectively) was observed compared to substrates **4a** and **3a** bearing a TIPS-substituent (entries 1 and 5, respectively). When comparing the energetic pathways for substrates **3a** ($\text{R} = \text{TIPS}$) and **3b** ($\text{R} = \text{Mes}$), an effect of the TIPS-moiety was observed on (i) *cis* \rightarrow *trans* isomerization and (ii) reductive elimination (Scheme 6). More specifically, the TIPS-group leads to a significant destabilization of $\text{Pd}(\text{u})$ intermediates **VI** and **V**, along with a stabilization of the transition state for *cis* \rightarrow *trans* isomerization, which causes a substantial decrease in the barrier of isomerization and overall results in a flatter energetic pathway and thus a smaller energetic span.

Steric effects of the silyl group. While for TIPS-substituted $\text{Pd}(\text{u})$ intermediates, the *trans*-intermediate **Va** is more stable than its corresponding *cis*-intermediate **VIa**, the opposite preference is observed for the mesityl-substituted $\text{Pd}(\text{u})$ intermediates, *i.e.* **VIb** is more stable than **Vb**. Overall, both $\text{Pd}(\text{u})$ intermediates **VIa** and **Va** are significantly destabilized by the TIPS-moiety compared to the corresponding mesityl-substituted intermediates (**VIb** and **Vb**). However, the degree of destabilization is more pronounced for the *cis*- $\text{Pd}(\text{u}) intermediate **VIa**. This would be in agreement with an increased steric interaction of the TIPS moiety with the aryl group of the oxindole in **VIa** compared to **Va**. In contrast, the mesityl moiety can rotate away (into a side-on conformation), in which there is significantly less steric interaction, thus rendering the Pd -substituent the most sterically congesting moiety. Therefore, the preference of **VIb** over **Vb** appears to be due to a decreased steric interaction of $\text{PdCl}(\text{PtBu}_3)$ with the aromatic backbone of the oxindole.⁴⁸$



Scheme 5 Ligand effect on alkyne chlorocarbamoylation of **3a**: calculated Gibbs free energy pathways employing $\text{L} = \text{PtBu}_3$ (blue, *italicics*) and $\text{L} = \text{PA-Ph}$ (green, **bold**). Energies (in kcal mol⁻¹) were calculated at the CPCM (toluene) M06L/def2-TZVP//B3LYP/6-31G(d)(LANL2DZ) level of theory.





Scheme 6 Effect of silyl substituent on the alkyne: calculated Gibbs free energy pathways of **3a** (R = TIPS, blue, bold) and **3b** (R = Mes, teal, *italics*) at the CPCM (toluene) M06L/def2-TZVP//B3LYP/6-31G(d)(LANL2DZ) level of theory (energies are given in kcal mol⁻¹)

Electronic effects of the silyl group. In order to investigate the nature of the *cis* → *trans* isomerization TS, we analyzed (i) the charge distribution in the Pd(II)-intermediates, **VIA** and **Va**, as well as during the isomerization TS and (ii) the change in bond lengths from *cis*-intermediate **VIA** *via* the TS to *trans*-intermediate **Va** (Fig. 2). For this reason, a natural bond order analysis (NBO analysis)^{54–57} was performed, which showed that only a minor change in charge separation occurs in the case of TIPS, whereas a significant buildup of charge separation takes place for R = Mes. More specifically, TIPS-substituted

intermediates **VIA** and **Va** already possess a high degree of charge separation with a positive charge of +0.53 on the silyl substituent and only a minor increase of 4% leads to the isomerization TS (positive charge of +0.55 on the silyl moiety). In contrast, mesityl-substituted intermediates do not exhibit significant charge separation (+0.03 and +0.08 on mesityl for intermediates **VIb** and **Vb**, respectively) and a substantial separation of charges needs to be established (increase of 136%) in order to reach the charge-separated TS (with a positive charge of +0.16 on mesityl). This analysis is in line with calculated Atoms-In-Molecules (AIM)⁵⁸ charges, which indicate essentially no change in charge on Si (increase of 0.2%) to reach the isomerization TS, but a strong increase in charge of 77% on the *ipso*-C of the mesityl-substituent in order to undergo isomerization.⁴⁸ These results are congruent with the observed energetic destabilization of TIPS-substituted Pd(II)-intermediates **VIA** and **Va** and indicate that the low barrier for *cis* → *trans* isomerization for R = TIPS is primarily a result of a destabilization of intermediates rather than a stabilization of the TS. Moreover, charge separation is much larger in the presence of the silyl substituent, suggesting that the TIPS-moiety can better stabilize charge buildup and thus lowers the barrier for the isomerization process.

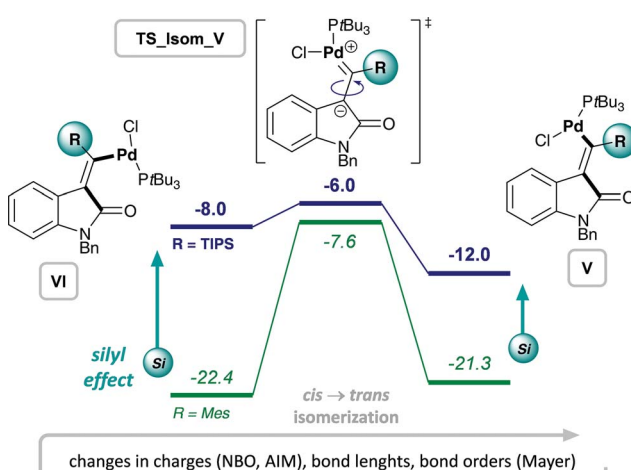
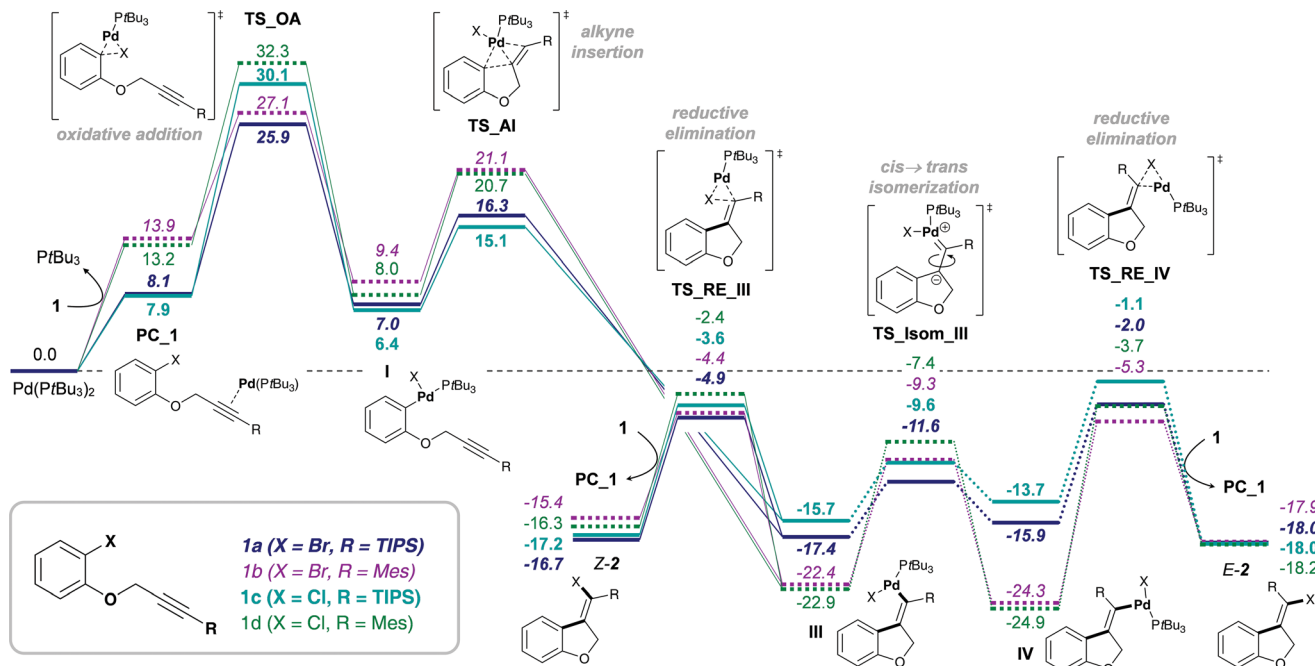


Fig. 2 Effect of alkyne substituent on Pd(II) intermediates, VI and V, and *cis* \rightarrow *trans* isomerization: analysis of charges, bond lengths and bond orders

This result is in agreement with the known effect of silyl groups to be able to stabilize carbocations in α ,⁵⁹ β ^{60,61} and γ ⁶² positions. In addition, analyzing the changes in bond lengths during the isomerization from *cis*- to *trans*-Pd(II) intermediate (**VIa** to **Va**) shows a slight elongation of the double bond and concomitant shortening of both C-Si and C-Pd bonds in the TS, suggesting a delocalization of positive charge between Pd, C,



Scheme 7 Gibbs free energy pathway of the $\text{Pd}(\text{PtBu}_3)_2$ -mediated alkyne carbohalogenation of **1a–d**, calculated at the CPCM (toluene) M06L/def2-TZVP//B3LYP/6-31G(d)(LANL2DZ) level of theory (values are given in kcal mol^{-1}).

and Si.⁴⁸ This corresponds with the calculated Mayer bond orders,^{63,64} which indicate a decrease in bond order of the $\text{C}=\text{C}$ double bond during the TS for both $\text{R} = \text{TIPS}$ and $\text{R} = \text{Mes}$, although more pronounced for the latter. At the same time, the $\text{C}-\text{R}$ ($\text{R} = \text{TIPS}$ or Mes) bond order increases during isomerization (indicating delocalization of charge into the R-substituent). This increase is only minor for the silyl moiety (increase of 8%), but more evident for mesityl (increase of 20%) as expected due to the bigger required changes in order to reach the TS.⁴⁸

Overall, the silyl moiety exerts a combination of effects on several intermediates and steps in the chlorocarbamoylation reaction, giving rise to its unique reactivity.

Origins of observed divergence in selectivity

In the reaction of carbamoyl chlorides an exclusive *E*-selectivity is reached by means of a rapid *cis* \rightarrow *trans* isomerization (see Scheme 1b). However, in the corresponding reaction of aryl halides medium to good levels of *Z*-selectivity are observed as a result of direct reductive elimination. In the case of mesityl substituted alkynes, a switch in selectivity (*i.e.* to obtain **E-2b**) can be reached at elevated reaction temperatures (see Scheme 1a). Additionally, the substrate scope is not limited to TIPS-substituted alkynes, tolerating other bulky groups, such as aryls for example.

Analysis of the calculated free energy pathways revealed a pronounced effect of the alkyne substituent on the reactivity profile (Scheme 7). Analogous to reactions of the amide-tethered substrates 3 and 4 (Schemes 4–6), a TIPS-substituent favors the *cis*-Pd(*ii*) intermediate **IIIa**, but the corresponding *trans*-intermediate **IV** is more stable when possessing a mesityl-

substituent (**IVb**). In addition, the barrier towards isomerization is significantly lower for $\text{R} = \text{TIPS}$ compared to $\text{R} = \text{Mes}$, *i.e.* $\Delta G^\ddagger = 5.8$ and $13.1 \text{ kcal mol}^{-1}$ for substrates **1a** ($\text{R} = \text{TIPS}$) and **1b** ($\text{R} = \text{Mes}$), respectively. Moreover, the stability of the pre-complexes **PC_1**, where the active monophosphine $\text{Pd}(0)(\text{PtBu}_3)$ species coordinates to the alkyne group of substrate **1**, is more pronounced when $\text{R} = \text{TIPS}$, indicating that the silyl group increases the electrophilic character of the alkyne moiety. This would suggest that the reductive elimination from the vinyl Pd(*ii*) intermediates, **III** and **IV**, is reversible for substrates **1b** and **1d** bearing a mesityl-substituent. In combination with the *trans*-Pd(*ii*) intermediate **IV** being more stable than the *cis*-intermediate **III**, a reversal of the observed *Z*-selectivity for $\text{R} = \text{Mes}$ (50°C) can be reached at elevated reaction temperatures (100°C).^{16,65}

Conclusions

The mechanisms of alkyne carbohalogenation and chlorocarbamoylation have been investigated by means of DFT calculations and experiments. Catalytic pathways involving oxidative addition, alkyne insertion, *cis* \rightarrow *trans* isomerization and reductive elimination are proposed. Oxidative addition is suggested to be reactivity limiting in the case of addition of aryl halides across alkynes: in the corresponding reaction of carbamoyl chlorides, oxidative addition was however shown to be fast and our data indicated that instead alkyne insertion, *i.e.* carbopalladation was reactivity limiting. Furthermore, the effects of halide, phosphine ligand and alkyne substituent on reactivity were investigated.

While the bulky PtBu_3 was vital for reactivity in the intramolecular addition of aryl halides across alkynes due to



a lowering of the barriers for reductive elimination, the less bulky phosphadamantane ligand PA-Ph is uniquely suited for the corresponding addition reaction of carbamoyl chlorides. Calculations indicate that this is due to a significant decrease in the barrier for the reactivity limiting alkyne insertion with the less bulky PA-Ph ligand compared to $PtBu_3$. Notably, a pronounced effect of the alkyne substituent on reactivity was unravelled, which accounts for the exceptional reactivity of substrates bearing a TIPS-substituent. More specifically, the bulky TIPS-group was shown to cause a significant destabilization of $Pd^{(II)}$ intermediates **VI** and **V**, along with a stabilization of the *cis* \rightarrow *trans* isomerization **TS**. This overall results in a smaller energetic span and thus significantly increases catalytic turnover.

Acknowledgements

F. S. and T. S. wish to thank the RWTH Aachen, MIWF NRW and the Evonik Foundation (doctoral scholarship to T. S.) for financial support and greatly appreciate the granted computing time on the RWTH Bull Cluster (grant number jara0091). M. L. thanks NSERC, the University of Toronto and Alphora Inc. for funding. C. M. L. thanks NSERC for a postgraduate scholarship.

Notes and references

- 1 S. T. Davis, S. H. Dickerson, S. V. Frye, P. A. Harris, R. N. Hunter, L. F. Kuyper, K. E. Lackey, M. J. Luzzio, J. M. Veal and D. H. Walker, Patent WO9915500, 1999.
- 2 A. Heckel, G. J. Roth, J. Kley, S. Hoerer and I. Uphues, Patent WO2005087727 A1, 2005.
- 3 S. Hauf, R. W. Cole, S. LaTerra, C. Zimmer, G. Schnapp, R. Walter, A. Heckel, J. van Meel, C. L. Rieder and J.-M. Peters, *J. Cell Biol.*, 2003, **161**, 281–294.
- 4 C. A. Grandinetti and B. R. Goldspiel, *Pharmacotherapy*, 2007, **27**, 1125–1144.
- 5 F. Hilberg, G. J. Roth, M. Krssak, S. Kautschitsch, W. Sommergruber, U. Tontsch-Grunt, P. Garin-Chesa, G. Bader, A. Zoephel, J. Quant, A. Heckel and W. J. Rettig, *Cancer Res.*, 2008, **68**, 4774–4782.
- 6 B. M. Trost, N. Cramer and H. Bernsmann, *J. Am. Chem. Soc.*, 2007, **129**, 3086–3087.
- 7 B. M. Trost, N. Cramer and S. M. Silverman, *J. Am. Chem. Soc.*, 2007, **129**, 12396–12397.
- 8 S. Lin and S. J. Danishefsky, *Angew. Chem., Int. Ed.*, 2001, **40**, 1967–1970.
- 9 G. Cantagrel, B. de Carné-Carnavalet, C. Meyer and J. Cossy, *Org. Lett.*, 2009, **11**, 4262–4265.
- 10 S. Tang, Q.-F. Yu, P. Peng, J.-H. Li, P. Zhong and R.-Y. Tang, *Org. Lett.*, 2007, **9**, 3413–3416.
- 11 M. Sassatelli, É. Debiton, B. Aboab, M. Prudhomme and P. Moreau, *Eur. J. Med. Chem.*, 2006, **41**, 709–716.
- 12 M. S. C. Pedras, J. L. Sorensen, F. I. Okanga and I. L. Zaharia, *Bioorg. Med. Chem. Lett.*, 1999, **9**, 3015–3020.
- 13 E. M. Beccalli and A. Marchesini, *Tetrahedron*, 1995, **51**, 2353–2362.
- 14 E. M. Beccalli, A. Marchesini and T. Pilati, *Tetrahedron*, 1994, **50**, 12697–12712.
- 15 C. M. Le, X. Hou, T. Sperger, F. Schoenebeck and M. Lautens, *Angew. Chem., Int. Ed.*, 2015, **54**, 15897–15900.
- 16 C. M. Le, P. J. C. Menzies, D. A. Petrone and M. Lautens, *Angew. Chem., Int. Ed.*, 2015, **54**, 254–257.
- 17 X. Jiang, H. Liu and Z. Gu, *Asian J. Org. Chem.*, 2012, **1**, 16–24.
- 18 *Higher Oxidation State Organopalladium and Platinum Chemistry*, ed. A. J. Canty, Springer-Verlag, Berlin Heidelberg, 2011.
- 19 A. J. Canty, *Acc. Chem. Res.*, 1992, **25**, 83–90.
- 20 A. J. Hickman and M. S. Sanford, *Nature*, 2012, **484**, 177–185.
- 21 K. M. Engle, T.-S. Mei, X. Wang and J.-Q. Yu, *Angew. Chem., Int. Ed.*, 2011, **50**, 1478–1491.
- 22 D. C. Powers and T. Ritter, *Nat. Chem.*, 2009, **1**, 302–309.
- 23 D. C. Powers, D. Benitez, E. Tkatchouk, W. a. Goddard and T. Ritter, *J. Am. Chem. Soc.*, 2010, **132**, 14092–14103.
- 24 D. C. Powers, E. Lee, A. Ariafard, M. S. Sanford, B. F. Yates, A. J. Canty and T. Ritter, *J. Am. Chem. Soc.*, 2012, **134**, 12002–12009.
- 25 D. Kalyani, A. R. Dick, W. Q. Anani and M. S. Sanford, *Org. Lett.*, 2006, **8**, 2523–2526.
- 26 K. J. Stowers and M. S. Sanford, *Org. Lett.*, 2009, **11**, 4584–4587.
- 27 P. L. Arnold, M. S. Sanford and S. M. Pearson, *J. Am. Chem. Soc.*, 2009, **131**, 13912–13913.
- 28 A. H. Roy and J. F. Hartwig, *J. Am. Chem. Soc.*, 2001, **123**, 1232–1233.
- 29 A. H. Roy and J. F. Hartwig, *J. Am. Chem. Soc.*, 2003, **125**, 13944–13945.
- 30 A. H. Roy and J. F. Hartwig, *Organometallics*, 2004, **23**, 1533–1541.
- 31 D. A. Watson, M. Su, G. Teverovskiy, Y. Zhang, J. García-Fortanet, T. Kinzel and S. L. Buchwald, *Science*, 2009, **325**, 1661–1664.
- 32 X. Shen, A. M. Hyde and S. L. Buchwald, *J. Am. Chem. Soc.*, 2010, **132**, 14076–14078.
- 33 D. A. Petrone, H. Yoon, H. Weinstabl and M. Lautens, *Angew. Chem., Int. Ed.*, 2014, **53**, 7908–7912.
- 34 M. J. Frisch, G. W. Trucks, H. B. Schlegel, G. E. Scuseria, M. A. Robb, J. R. Cheeseman, G. Scalmani, V. Barone, B. Mennucci, G. A. Petersson, H. Nakatsuji, M. Caricato, X. Li, H. P. Hratchian, A. F. Izmaylov, J. Bloino, G. Zheng, J. L. Sonnenberg, M. Hada, M. Ehara, K. Toyota, R. Fukuda, J. Hasegawa, M. Ishida, T. Nakajima, Y. Honda, O. Kitao, H. Nakai, T. Vreven, J. A. Montgomery Jr, J. E. Peralta, F. Ogliaro, M. Bearpark, J. J. Heyd, E. Brothers, K. N. Kudin, V. N. Staroverov, T. Keith, R. Kobayashi, J. Normand, K. Raghavachari, A. Rendell, J. C. Burant, S. S. Iyengar, J. Tomasi, M. Cossi, N. Rega, J. M. Millam, M. Klene, J. E. Knox, J. B. Cross, V. Bakken, C. Adamo, J. Jaramillo, R. Gomperts, R. E. Stratmann, O. Yazyev, A. J. Austin, R. Cammi, C. Pomelli, J. W. Ochterski, R. L. Martin, K. Morokuma, V. G. Zakrzewski, G. A. Voth, P. Salvador, J. J. Dannenberg, S. Dapprich, A. D. Daniels, O. Farkas, J. B. Foresman,



J. V. Ortiz, J. Cioslowski, and D. J. Fox, *Gaussian 09, Revision D.01*, Gaussian, Inc., Wallingford CT, 2013.

35 For appropriateness of computational method, see: T. Sperger, I. A. Sanhueza, I. Kalvet and F. Schoenebeck, *Chem. Rev.*, 2015, **115**, 9532–9586.

36 Y. Lan, P. Liu, S. G. Newman, M. Lautens and K. N. Houk, *Chem. Sci.*, 2012, **3**, 1987–1995.

37 S. G. Newman and M. Lautens, *J. Am. Chem. Soc.*, 2011, **133**, 1778–1780.

38 C. L. McMullin, N. Fey and J. N. Harvey, *Dalton Trans.*, 2014, **43**, 13545–13556.

39 C. L. McMullin, J. Jover, J. N. Harvey and N. Fey, *Dalton Trans.*, 2010, **39**, 10833–10836.

40 K. Vikse, T. Naka, J. S. McIndoe, M. Besora and F. Maseras, *ChemCatChem*, 2013, **5**, 3604–3609.

41 M. Besora, C. Gourlaouen, B. Yates and F. Maseras, *Dalton Trans.*, 2011, **40**, 11089–11094.

42 F. Barrios-Landeros, B. P. Carrow and J. F. Hartwig, *J. Am. Chem. Soc.*, 2009, **131**, 8141–8154.

43 M. Ahlquist and P.-O. Norrby, *Organometallics*, 2007, **26**, 550–553.

44 M. Ahlquist, P. Fristrup, D. Tanner and P.-O. Norrby, *Organometallics*, 2006, **25**, 2066–2073.

45 H. M. Senn and T. Ziegler, *Organometallics*, 2004, **23**, 2980–2988.

46 T. Sperger, H. C. Fisher and F. Schoenebeck, *Wiley Interdiscip. Rev.: Comput. Mol. Sci.*, 2016, **6**, 226–242.

47 F. Proutière and F. Schoenebeck, *Angew. Chem., Int. Ed.*, 2011, **50**, 8192–8195.

48 Please see ESI† for further details.

49 Calculations are in line with the experiment and predict a difference in activation barriers of oxidative addition of $\Delta\Delta G^\ddagger = 8.3$ kcal mol⁻¹ in favor of carbamoyl chloride activation.

50 An ionic, nucleophilic addition TS could not be located owing to the difficulties associated with the description of charges, which represent a well-known challenge. For further information, please refer to ref. 46.

51 C. Amatore and A. Jutand, *J. Organomet. Chem.*, 1999, **576**, 254–278.

52 S. Kozuch and S. Shaik, *Acc. Chem. Res.*, 2011, **44**, 101–110.

53 Notably, catalyst decomposition was observed via ³¹P NMR, no Pd(PtBu₃)₂ or free PtBu₃ were remaining after the reaction.

54 J. P. Foster and F. Weinhold, *J. Am. Chem. Soc.*, 1980, **102**, 7211–7218.

55 A. E. Reed, R. B. Weinstock and F. Weinhold, *J. Chem. Phys.*, 1985, **83**, 735–746.

56 A. E. Reed and F. Weinhold, *J. Chem. Phys.*, 1985, **83**, 1736–1740.

57 A. E. Reed, L. A. Curtiss and F. Weinhold, *Chem. Rev.*, 1988, **88**, 899–926.

58 R. F. W. Bader, *Atoms in Molecules: A Quantum Theory*, Oxford University Press, New York, 1990.

59 A. Kostenko, B. Müller, F.-P. Kaufmann, Y. Apeloig and H.-U. Siehl, *Eur. J. Org. Chem.*, 2012, 1730–1736.

60 K. C. Sproul and W. A. Chalifoux, *Org. Lett.*, 2015, **17**, 3334–3337.

61 T. Nokami, Y. Yamane, S. Oshitani, J.-k. Kobayashi, S.-i. Matsui, T. Nishihara, H. Uno, S. Hayase and T. Itoh, *Org. Lett.*, 2015, **17**, 3182–3185.

62 X. Creary and E. D. Kochly, *J. Org. Chem.*, 2009, **74**, 9044–9053.

63 I. Mayer, *Chem. Phys. Lett.*, 1983, **97**, 270–274.

64 I. Mayer, *Chem. Phys. Lett.*, 2012, **544**, 83–86.

65 Observed selectivities for substrate **1b** (X = Br, R = Mes), determined by ¹H NMR analysis of the crude reaction mixture using 1,3,5-trimethoxybenzene as an internal standard after reaction for 18 h in toluene (0.1 M) employing 5 mol% Pd(QPhos)₂: Z/E > 95 : 5 at 50 °C and 10 : 90 at 100 °C.

